Protein–protein interactions between jasmonate-related master regulator MYC and transcriptional mediator MED25 depend on a short binding domain

Received for publication, September 13, 2021, and in revised form, December 11, 2021 Published, Papers in Press, December 18, 2021,
https://doi.org/10.1016/j.jbc.2021.101504

Yousuke Takaoka[1,*], **Kaho Suzuki**[1], **Akira Nozawa**[2], **Hirotaka Takahashi**[2], **Tatsuya Sawasaki**[2], and **Minoru Ueda**[1,3,*]

From the [1]*Department of Chemistry, Graduate School of Science, Tohoku University, Sendai, Japan;* [2]*Proteo-Science Center (PROS), Ehime University, Matsuyama, Ehime, Japan;* [3]*Department of Molecular and Chemical Life Sciences, Graduate School of Life Sciences, Tohoku University, Sendai, Japan*

Edited by Joseph Jez

A network of protein–protein interactions (PPI) is involved in the activation of (+)-*7-iso*-jasmonoyl-L-isoleucine (JA-Ile), a plant hormone that regulates plant defense responses as well as plant growth and development. In the absence of JA-Ile, inhibitory protein jasmonate-ZIM-domain (JAZ) represses JA-related transcription factors, including a master regulator, MYC. In contrast, when JA-Ile accumulates in response to environmental stresses, PPI occurs between JAZ and the F-box protein COI1, which triggers JAZ degradation, resulting in derepressed MYC that can interact with the transcriptional mediator MED25 and upregulate JA-Ile-related gene expression. Activated JA signaling is eventually suppressed through the catabolism of JA-Ile and feedback suppression by JAZ splice variants containing a cryptic MYC-interacting domain (CMID). However, the detailed structural basis of some PPIs involved in JA-Ile signaling remains unclear. Herein, we analyzed PPI between MYC3 and MED25, focusing on the key interactions that activate the JA-Ile signaling pathway. Biochemical assays revealed that a short binding domain of MED25 (CMIDM) is responsible for the interaction with MYC, and that a bipartite interaction is critical for the formation of a stable complex. We also show the mode of interaction between MED25 and MYC is closely related to that of CMID and MYC. In addition, quantitative analyses on the binding of MYC3-JAZs and MYC3-MED25 revealed the order of binding affinity as $JAZ^{Jas} < MED25^{CMIDM} < JAZ^{CMID}$, suggesting a mechanism for how the transcriptional machinery causes activation and negative feedback regulation during jasmonate signaling. These results further illuminate the transcriptional machinery responsible for JA-Ile signaling.

(+)-7-*iso*-jasmonoyl-L-isoleucine (JA-Ile) is an oxylipin-derived plant hormone that regulates plant defense responses and growth (1, 2). In its absence, JA-Ile responses are restrained by a group of transcriptional repressors called "jasmonate-ZIM-domain" (JAZ) proteins. In *Arabidopsis thaliana*, a conserved C-terminal Jas motif of JAZ proteins physically interacts with and inhibits basic helix–loop–helix transcription factors (TFs), including MYC2, MYC3, and MYC4. In addition, JAZ proteins recruit TOPLESS (TPL) as a corepressor either through direct binding of TPL to ethylene-response factor-associated amphiphilic repression motifs at the N terminus of JAZ proteins, or indirectly through the ethylene-response factor-associated amphiphilic repression motif-containing NOVEL INTERACTOR OF JAZ (NINJA) adaptor protein that binds to the central ZIM domain of JAZ proteins (3–6). JA-Ile is quickly biosynthesized in response to internal or external cues and then induces the protein–protein interaction (PPI) between F-box protein CORONATINE INSENSITIVE 1 (COI1) and JAZ, which triggers ubiquitination and subsequent degradation of the JAZ through the *26S*-proteasome (7–10). Thereafter, the derepressed MYC TFs can physically interact with the transcriptional mediator MED25, recruiting the histone acetyl transferase1 to the target promoters of MYC and bridging MYC and the RNA polymerase II for transcriptional preinitiation complex assembly, upregulating various JA-Ile-related genes (Fig. 1) (11–16). Activated jasmonate signaling is eventually suppressed through two independent mechanisms: catabolism of JA-Ile by CYP94B1/B3/C1 monooxygenases (17–19) and feedback suppression of jasmonate signaling through the expression of JAZ10 splice variants, such as JAZ10.3 (lacking the C terminus of Jas motif), JAZ10.4 (lacking the entire Jas motif), and JAZ10.1 (full-length JAZ10). These splice variants contain an N-terminal cryptic MYC-interaction domain (CMID) that interacts with MYC proteins to repress the MYC target gene expression. Because the increase of JA-Ile level causes accumulation of JAZ10.4 protein, JAZ10 splice variants are considered to be the important negative feedback regulators of JA signaling (20–23). However, with the exception of COI1-JAZ and JAZ-MYC, the detailed structural basis of PPIs involved in jasmonate signaling remains unclear (21, 24, 25). For example, 407 to 680aa of MED25 was reported to participate in the binding with MYC3, however, the detailed mode of binding has not been clarified (25).

Here, we report a biochemical analysis of the mode of PPI between MYC and MED25. We conclude that a short-binding

* For correspondence: Minoru Ueda, minoru.ueda.d2@tohoku.ac.jp; Yousuke Takaoka, ytakaoka@tohoku.ac.jp.

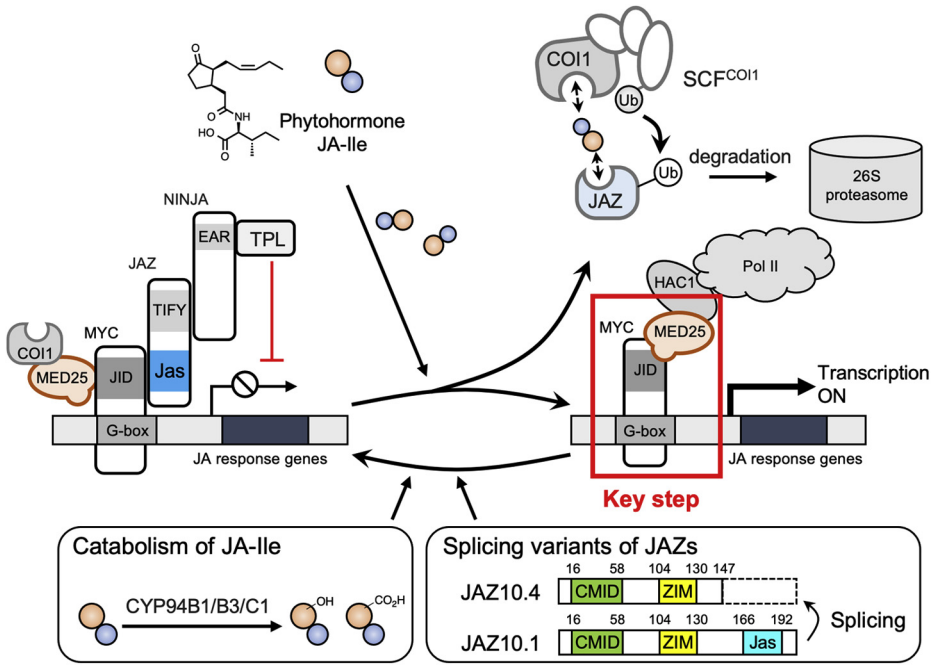

Figure 1. Schematic of the resting stage (*left*) and MED25-mediated activation stage (*right*) in the JA signaling. In the resting stage, Jas motif of JAZ protein physically interacts with MYC and/or recruit TPL through EAR motifs-containing NINJA adapter protein for the suppression of JA response genes expression. In the activation stage, JA-Ile induces PPI between COI1/JAZ, which triggers degradation of the JAZ through the *26S*-proteasome (*upper right*), and thereafter, the derepressed MYC physically interact with MED25, recruiting HAC1 and Pol II for the upregulation of various JA responsive genes expression. CMID, cryptic MYC-interacting domain; COI1, CORONATINE INSENSITIVE 1; EAR, ethylene-response factor-associated amphiphilic repression; JA-Ile, (+)-7-iso-jasmonoyl-L-isoleucine; JAZ, jasmonate-ZIM-domain; NINJA, NOVEL INTERACTOR OF JAZ; Pol II, polymerase II; PPI, protein–protein interaction; TPL, TOPLESS.

domain of MED25 is responsible for the interaction with MYC, and the mode of interaction between MED25 and MYC is similar to that of CMID and MYC. These findings give new insights into the structural basis of jasmonate signaling machinery.

Results

AlphaScreen assay of protein–protein interaction between MYC3 and MED25

A previous study by Zhang *et al.* mapped the interaction domain of MED25 with MYC3 to a large region (amino acids 407–680) and includes the MED25 activator interaction domain (25). To investigate the PPI between MED25 and MYC3, we constructed a wheat germ-derived cell-free translation system for full-length MYC proteins bearing a FLAG tag (FLAG-MYC2, 3, 4) and a MED25 (407–680 aa) protein bearing a GST tag and biotin-ligation site (Bls) sequence (GST-Bls-MED25) and studied them using the AlphaScreen technique, as previously described (Figs. 2*A* and S1) (26, 27). A full-length JAZ9 protein bearing a GST tag and Bls sequence (GST-Bls-JAZ9) was also constructed for comparison (Figs. 2*A* and S1). In the AlphaScreen assay, the reaction mixture containing FLAG-MYC and GST-Bls-MED25 or GST-Bls-JAZ9 was initially incubated for 2 h at 4 °C. Subsequently, anti-FLAG antibody-coated AlphaScreen acceptor beads and Streptavidin-coated donor beads were added to each sample, and the mixture was incubated for 5 h at room temperature. On laser excitation, a photosensitizer in the donor bead converts ambient oxygen to a more excited singlet state. In the case of interaction between two proteins and the resulting proximity of the two beads, the singlet state oxygen molecules diffuse across to react with the acceptor bead generating chemiluminescence light (Fig. S1*A*). In contrast, in the absence of a specific interaction between two proteins, the singlet state oxygen molecules produced by the donor bead go undetected without the close proximity of the acceptor bead, resulting in the production of a very low background signal. As shown in Figure 2*B*, the samples containing FLAG-MYC3 and GST-Bls-MED25 had a high signal intensity of the AlphaScreen compared with MYC3 alone, indicating that full-length MYC3 directly interacts with MED25 *in vitro,* as previously reported (25).

Previous studies of the crystal structure of MYC3-JAZ9 identified the amino acid residues L125, E148, F151, L152, and M155 of MYC3 as being important for interaction with JAZ9 (25). We prepared the alanine or arginine mutants of these amino acids to examine the interaction mode between MYC3 and MED25 (Fig. S2). As previously reported, the affinities of these MYC3 mutants for JAZ9 (Fig. 2*C*) were minimal, whereas their affinities for MED25 were similar or slightly lower than that of WT MYC3 (Fig. 2*B*). The affinities for MED25 of mutants incorporating alanine in place of the hydrophobic amino acids F151, L152, and M155 were slightly decreased. Therefore, we next evaluated the affinities of double mutants of these peptides, L125A/F151A, L125A/

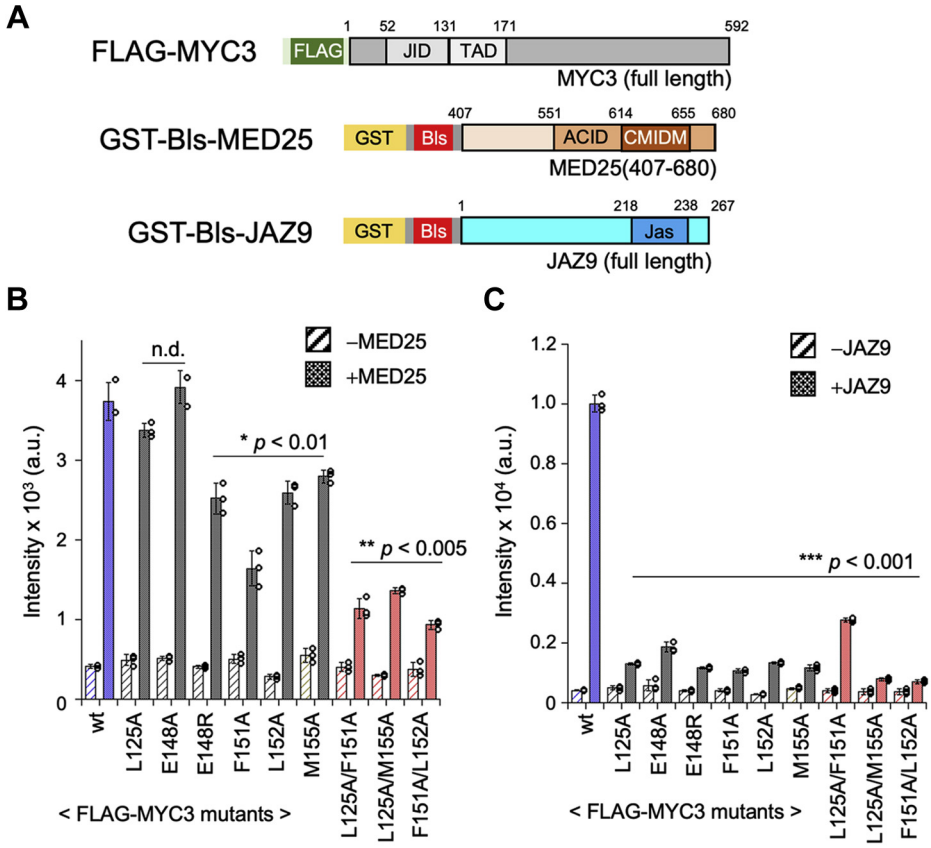

Figure 2. AlphaScreen analyses of the protein-protein interactions between FLAG-MYC3 and GST-Bls-MED25. *A,* schematic representation of each protein construct used in the AlphaScreen assay; FLAG-MYC3: FLAG-tagged full-length MYC3, GST-Bls-MED25: GST- and biotin-ligase substrate sequence (Bls)-tagged MED25 (407–680) containing ACID (551–680) and CMIDM (614–655), and GST-Bls-JAZ9: GST- and Bls-tagged full length JAZ9. *B* and *C,* AlphaScreen analyses of the protein–protein interactions between (*B*) FLAG-MYC3 (wt or Ala mutants, 50 nM) and GST-Bls-MED25 (150 nM) or (*C*) FLAG-MYC3 (wt or Ala mutants, 50 nM) and GST-Bls-JAZ9 (150 nM). The experiments were performed in triplicate to obtain mean values with SD (shown as error bars). The *asterisks* represent significant differences between signal intensity of wt-MYC3/MED25 or wt-MYC3/JAZ9 and that of mutated-MYC3/MED25 or mutated-MYC3/JAZ9 and were evaluated by Students' *t* test (*$p < 0.01$, **$p < 0.005$, ***$p < 0.001$). Bls, biotin-ligation site; CMIDM, CMID-like MYC-interacting domain; JAZ, jasmonate-ZIM-domain; JID, the JAZ-interacting domain; TAD, the transcription activation domain.

M155A, and F151A/L152A (Fig. S3). As was the case for JAZ9, their affinities for MED25 were all significantly decreased (Fig. 2, *B* and *C*), suggesting that the hydrophobic interactions between MED25 and more than one amino acid of MYC3 are crucial for their interaction. This interaction between MED25 and MYC3 was clearly different from that of MYC3-JAZ9^{Jas}. However, close mode of interaction can be found in the interaction between MYC3 and JAZ10^{CMID}, in which the CMID of JAZ10 is involved in rerepression of MYC (20, 21).

Identification of the interaction domain of MED25 with MYC

It is reported that the CMID of JAZ10 is also conserved in JAZ1, 2, 5, and 6 (21). Therefore, we next examined the homology between MED25 and these CMID regions. Of the MYC3-interacting domains of MED25 (amino acids 407–680) previously reported, the domain comprising amino acids 614 to 655 of MED25 is moderately homologous (21%) with the CMID regions (Fig. 3*A*), and so we named this domain the "CMID-like MYC-interacting domain" (CMIDM). To examine the role of CMIDM in the interaction between MED25 and MYC, we prepared MED25 mutants incorporating alanine in place of the highly conserved amino acids in the CMIDM and CMID sequences (S627A, K638A, P647A, and L653A, Fig. S4) and selected MED25 double mutants (S627A/K638A, S627A/P647A, S627A/L653A, K638A/L653A, K638A/L653A, and P647A/L653A, Fig. S5). As shown in Figure 3*B*, a significant decrease was observed in the signal intensities on AlphaScreen analyses, suggesting that most of the MED25 mutants have weaker affinities for MYC3 compared with WT MED25. Furthermore, a marked decrease of binding for MYC3 was observed for CMIDM-deletion mutant of MED25 (ΔCMIDM) (Figs. 3*C* and S6), indicating that CMIDM significantly contributes to the binding between MYC3 and MED25. Based on these findings, we prepared the biotin-conjugated CMIDM peptide of MED25 (614–655) (Biotin-MED25^{CMIDM}) (Figs. 4*A* and S7) for further analyses. In the AlphaScreen assay, this was demonstrated to directly interact with MYC3 (Fig. 4*B*). Moreover, it was revealed that Biotin-MED25^{CMIDM} has affinity for MYC2 or MYC4 and the MED25 protein (GST-Bls-MED25 (407–680aa) Fig. 4*C*). These results suggested that the CMIDM is an interacting domain of MED25 with the MYC TFs.

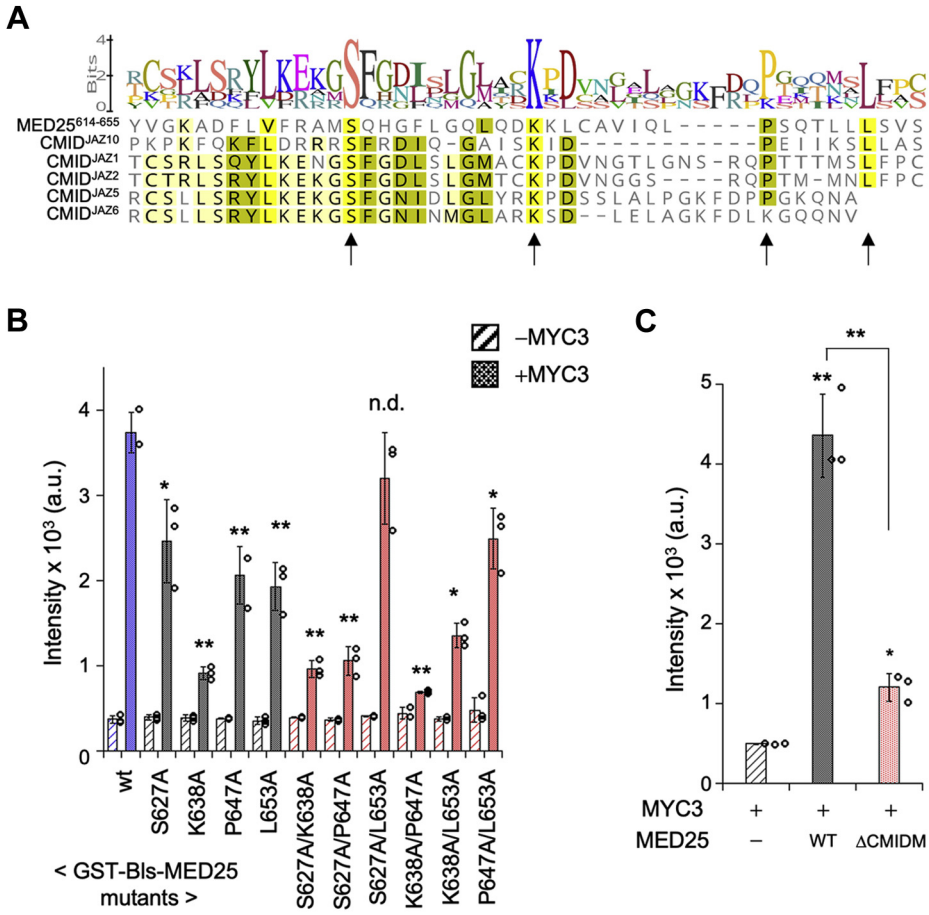

Figure 3. AlphaScreen analyses of the protein–protein interactions between FLAG-MYC3 and mutants of GST-Bls-MED25. *A,* sequence logos of MED25 (614–655) and various CMID of JAZ proteins (JAZ10^{CMID}, JAZ1^{CMID}, JAZ2^{CMID}, JAZ5^{CMID}, and JAZ6^{CMID}, respectively), created by Geneious 2019.2.1. The *arrowheads* indicated highly conserved amino acids in these sequences. *B,* AlphaScreen analyses of the protein–protein interaction between GST-Bls-MED25 (wt or Ala mutants, 150 nM) in the absence or presence of FLAG-MYC3 (50 nM). The experiments were performed in triplicate to obtain mean values with SD (shown as error bars). The *asterisks* represent significant differences between signal intensity of MYC3/wt-MED25 and that of MYC3/mutated-MED25 were evaluated by Students' *t* test (*$p < 0.01$, **$p < 0.005$). *C,* AlphaScreen analyses of the protein–protein interaction between FLAG-MYC3 (50 nM) in the absence or presence of GST-Bls-MED25 (WT or ΔCMIDM, 150 nM). The experiments were performed in triplicate to obtain mean values with SD (shown as error bars). The *asterisks* represent significant differences between the signal intensity of each mutant and that of wt-GST-Bls-MED25 with MYC3 and were evaluated by Students' *t* test (*$p < 0.01$, **$p < 0.005$). Bls, biotin-ligation site; CMID, cryptic MYC-interacting domain; CMIDM, CMID-like MYC-interacting domain; JAZ, jasmonate-ZIM-domain.

Quantitative binding affinity between MYC3 and its binding partners JAZ, MED25, and CMID

We next examined the binding affinity of MYC3 for its binding partners. As previously reported, a fluorescence anisotropy (FA) assay can be used to quantitatively assess the binding between the JAZ-binding domain of MYC3 (His6-SUMO-tagged MYC3 (44–238)) and fluorophore-conjugated JAZ-Jas motif peptide (28). Accordingly, we prepared the fluorescein-conjugated binding domains of MED25 and CMID (Fl-MED25^{CMIDM} and Fl-JAZ10^{CMID}, Figs. 5*A* and S8). Briefly, MYC3 protein solution was added dropwise to the solution containing Fl-MED25^{CMIDM} or Fl-JAZ10^{CMID}, and FA values were monitored by using fluorescence spectrometer with polarizers. As the results, the FA values of these peptides were significantly increased upon addition of His6-SUMO-MYC3 in dose-dependent manner, similar to the previously reported complex of fluorophore-conjugated JAZ9^{Jas} (TMR-JAZ9^{Jas}) and His6-SUMO-MYC3 (Fig. 5, *B* and *C*). The apparent K_d value of Fl-MED25^{CMIDM} was calculated to be 1.9 μM (Fig. 5*B*), which is significantly lower than that corresponding to TMR-JAZ9^{Jas} and MYC3 (5.0 μM) (28). In contrast, the K_d value of Fl-JAZ10^{CMID} was 0.47 μM (Fig. 5*C*), which is 3.6-fold lower than that of Fl-MED25^{CMIDM} and 10-fold lower than that of TMR-JAZ9^{Jas} (Fig. 6). These results indicate that CMID has a stronger binding affinity for MYC than both the Jas motif of JAZ and MED25, consistent with previous reports (21).

Discussion

The mechanism by which the transcriptional activation associated with JA-Ile signaling occurs is believed to be because of the changes in the combination of the various protein–protein interactions, based on recent reports of the genetic regulators involved in JA-Ile signaling. Here, we analyzed *in vitro* the protein–protein interactions between MYC3 and MED25, a key step in the activation of the JA-Ile signaling (Fig. 1). Using alanine mutants of MYC3, we revealed that the PPI between MYC3 and MED25 are predominantly reliant on a different mode-of-interaction from

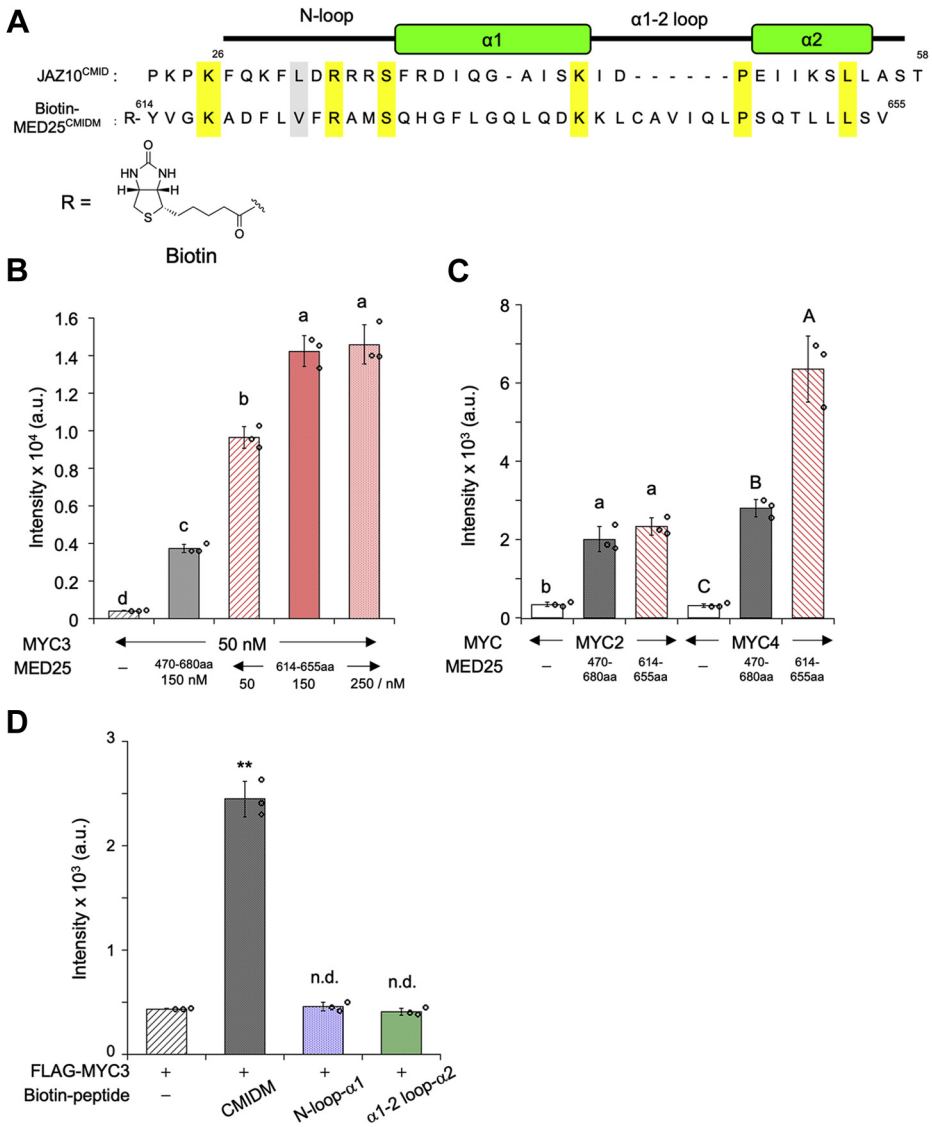

Figure 4. AlphaScreen analyses of the protein–peptide interactions between FLAG-MYC family and biotin-conjugated CMIDM peptide. *A,* chemical structures and amino acid sequences of JAZ10^{CMID} and biotin-conjugated CMIDM (614–655aa, Biotin-MED25^{CMIDM}). *B,* AlphaScreen analyses of FLAG-MYC3 (50 nM) with or without GST-Bls-MED25 (150 nM) or Biotin-MED25^{CMIDM} (50, 150, or 250 nM). *C,* AlphaScreen analyses of FLAG-MYC2 or FLAG-MYC4 (50 nM) with or without GST-Bls-MED25 (150 nM) or Biotin-MED25^{CMIDM} (150 nM). *D,* AlphaScreen signal intensity of FLAG-MYC3 (50 nM) in the absence and presence of Biotin-MED25^{CMIDM}, Biotin-MED25$^{N\text{-loop-}\alpha1}$, or Biotin-MED25$^{\alpha1\text{-}2\ loop-\alpha2}$ (150 nM each). The experiments were performed in triplicate to obtain mean values with SD (shown as error bars). In (*B*) and (*C*), significant differences were evaluated by one-way ANOVA/Tukey HSD post hoc test ($p < 0.01$). In (*D*), the *asterisks* represent significant differences between the signal intensity of each peptide and that of mock condition with MYC3 and were evaluated by Students' *t* test (*$p < 0.01$, **$p < 0.005$). Bls, biotin-ligation site; CMID, cryptic MYC-interacting domain; CMIDM, CMID-like MYC-interacting domain; JAZ, jasmonate-ZIM-domain.

those associated with the interaction between MYC3 and JAZ9 (Fig. 2) (21, 25). Furthermore, by using mutated MED25, we assigned the interaction domain of MED25 with MYC3 (CMIDM) (Figs. 3 and 4). The interaction between MYC3 and CMIDM was confirmed by canonical assays for protein–protein interaction, such as AlphaScreen (Fig. 4*B*), FA assay, (Fig. 5*B*), and pull down (Figs. S9 and S10). Our current results demonstrate that CMIDM contributes to the interaction between MED25 and MYC2/3/4 TFs (Fig. 4*C*) (12).

Previous reports have shown that JAZ10-CMID has a clamp-like twin-loop–helix structure bent at the proline48 (N-loop–α1–α1-2 loop–α2, Fig. S11), which interacts with both the Jas-binding groove and the backside of the Jas-interaction domain of MYC3 (21). Therefore, we prepared a biotin-conjugated partial peptide of CMIDM consisting of the part corresponding to N-loop–α1 in CMID (Biotin-MED25$^{N\text{-loop}-\alpha1}$) or α1-2 loop–α2 in CMID (Biotin-MED25$^{\alpha1\text{-}2\ loop-\alpha2}$) (Fig. S12, *A–E*) and investigated the contribution of binding to MYC3. As shown in Figure 4*D*, almost no interaction was observed in AlphaScreen analyses testing for interaction between N-loop–α1 or α1-2 loop–α2 and FLAG-MYC3, whereas a strong interaction was observed between Biotin-MED25^{CMIDM} peptide and FLAG-MYC3. These results imply that the bipartite interaction between CMIDM and MYC3 is critical for the formation of a stable complex. Previous reports also showed that MED25 interacts with not only the MYC family, but also various TFs belonging to the AP2/ERF TFs (OCTADECANOID-RESPONSIVE

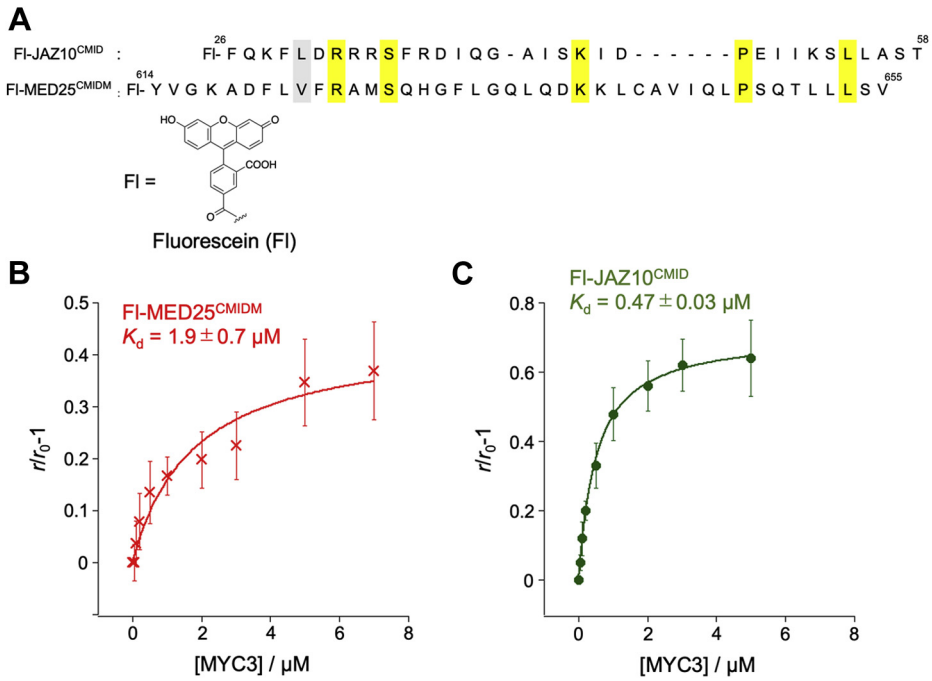

Figure 5. Quantitative analyses on the binding of MYC3-MED25 and MYC3-JAZ. *A*, chemical structures and amino acid sequences of fluorescein-conjugated JAZ10^{CMID} (26–58aa, Fl-JAZ10^{CMID}) and MED25^{CMIDM} (614–655aa, Fl-MED25^{CMIDM}). *B* and *C*, fluorescent anisotropy experiments of Fl-MED25^{CMIDM} (*B*, 50 nM) or Fl-JAZ10^{CMID} (*C*, 50 nM) with the addition of His6-SUMO-MYC3 (44–238) (0–7.5 μM). The experiments were performed in triplicate to obtain mean values with SD (shown as error bars). CMID, cryptic MYC-interacting domain; CMIDM, CMID-like MYC-interacting domain; JAZ, jasmonate-ZIM-domain.

ARABIDOPSIS AP2/ERF59 (ORA59), ethylene-responsive factor (ERF)), MYB, WRKY, bZIP, and zinc-finger TF families, indicating that MED25 acts as an integrator in the numerous steps in the JA-related transcriptional cascade (11, 12, 29, 30). These results provide structural insights into these complexes and could lead to elucidation of the switching mechanism between suppression and activation of JA-related transcription factors.

Furthermore, quantitative analyses by FA revealed the order of binding affinity between MYC3 and the partner proteins as JAZ^{Jas} < MED25^{CMIDM} < JAZ^{CMID}. In the AlphaScreen-based competitive assay for TMR-JAZ9^{Jas} with the complex of MYC3

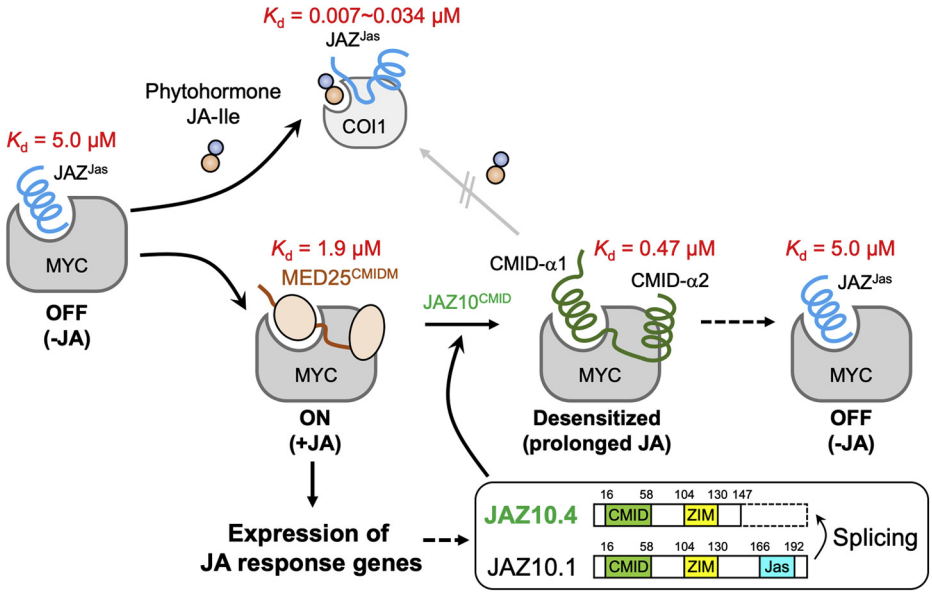

Figure 6. Schematic of JAZ, MED25, and CMID-mediated activation and desensitization mechanism of MYC in JA responses. When accumulation of JA-Ile, it induces PPI between COI1/JAZ^{Jas} (*upper right*), which triggers degradation of JAZ and interaction of MED25 and MYC (ON, +JA). Then, subsequent expression of *JAZ10.4* causes suppression of the gene expressions (desensitized and prolonged JA) and finally return to steady state (OFF, -JA). K_d values of these protein–peptide interactions between MYC3 and its binding partners or COI1–JA-Ile–JAZ are also included (28, 32). CMID, cryptic MYC-interacting domain; COI1, CORONATINE INSENSITIVE 1; JA-Ile, (+)-7-iso-jasmonoyl-L-isoleucine; JAZ, jasmonate-ZIM-domain; PPI, protein–protein interaction.

and MED25^{CMIDM} or biotin-MED25^{CMIDM} with the complex of MYC3 and JAZ10^{CMID}, these peptides competitively inhibited the corresponding complex dose-dependently (Fig. S13). These results suggested that the three binding domains belonging to JAZ (Jas motif and CMID) or MED25 (CMIDM) competitively bind to the same interacting site on MYC3. This order suggested that MED25^{CMIDM} can replace the position of JAZ^{Jas} in MYC3-JAZ^{Jas} complex, and the resulting MYC3-MED25^{CMIDM} can be replaced subsequently by JAZ^{CMID} to form MYC3–JAZ^{CMID} complex. These results strongly support the previously proposed picture of how the formation and transformation of transcriptional machinery in jasmonate signaling cause negative feedback regulation. The formation of COI1–JA-Ile–JAZ triggers degradation of JAZ repressor to upregulate the expression of *MED25* (11–13, 15, 16), and then subsequent expression of *JAZ* including the CMID sequence cause suppression of the gene expressions in jasmonate signaling (Fig. 6) (20, 21). Overall, revealing the MED25-mediated activation or desensitization mechanism of JA-Ile-related transcription factors would be an important step for not only clarifying the control mechanism of the entire jasmonate signaling, but leading to development of the specific chemical tools for JA-Ile related TFs in the future (28).

Experimental procedures

General materials and methods

All chemical reagents and solvents were obtained from commercial suppliers (Wako Pure Chemical Industries Co. Ltd, Nacalai Tesque Co., Ltd, Watanabe Chemical Industries Co. Ltd, Thermo Fisher Scientific K.K., and GE Healthcare) and used without further purification. DNA purification was accomplished using a GENE PREP STAR PI-80X DNA isolation system (KURABO). SDS-PAGE and Western blotting were performed using Mini-Protean III (Bio-Rad Laboratories, Inc.), Trans-Blot Turbo (Bio-Rad Laboratories, Inc.), and iBind Flex (Thermo Fisher Scientific) devices. Chemiluminescent images were detected using the Amersham Imager 680 detector (GE Healthcare). Reverse-phase HPLC was performed on a PU-4180 plus equipped with UV-4075 and MD-4010 detectors (JASCO). The absorbance at 220 nm and 488 nm was monitored by an MD-4010 photodiode array detector (PDA). MALDI-TOF MS analysis was performed on an Autoflex II (Bruker Daltonics Inc.).

Preparations of FLAG-MYC and GST-Bls-MED25 proteins

Standard methods for cloning were used, and all the PCR-amplified DNA fragments were sequenced after cloning into the vectors. The coding sequences of MYC2, 3, and 4 were provided by the RIKEN BRC through the National Bio-Resource Project of the MEXT/AMED, (pda00106 for MYC2 (AT1G32640), pda90611 for MYC3 (AT5G46760), and pda15392 for MYC4 (AT5G46830)). The plasmids for MYC2 and MYC4 are categorized to RIKEN Arabidopsis full-length cDNA clones (RAFL clones), which are inserted into modified pBluescript, and these plasmids were used as they were in the subsequent cell-free translation system. The plasmid for MYC3 is categorized to Arabidopsis Transcription factor clones (TF clones), which is inserted into pENTR207. Because the stop codon is missing in the TF clone, the MYC3 sequence was amplified by PCR with the addition of the stop codon and the restriction enzymes sites (EcoRV and BamHI, Table S1) and inserted into the pEU-E01-FLAG-MCS vector to generate pEU-E01-FLAG-MYC3. The coding sequences of MED25 (407–680aa) were isolated from Arabidopsis cDNA using the primers with the addition of the restriction enzymes sites (BamHI and SpeI, Table S1) and inserted into pEU-E01-GST-Bls-MCS vector to generate pEU-E01-GST-Bls-MED25. Site-directed mutagenesis of FLAG-MYC3 and GST-Bls-MED25 was performed based on the conventional inverse-PCR method with each primer (Tables S2 and S3). L125A/F151A, F125A/F151A, and F151A/L152A mutants of FLAG-MYC3 were amplified based on the plasmid of FLAG-MYC3 (F151A) mutant with corresponding primers. S627A/K638A and S627A/P647A mutants of GST-Bls-MED25 were amplified based on the plasmid of GST-Bls-MED25 (S627A) mutant with corresponding primers. K638A/P647A mutant of GST-Bls-MED25 was amplified based on the plasmid of GST-Bls-MED25 (K638A) mutant with corresponding primers. S627A/L653A, K638A/L653A, and P647A/L653A mutants of GST-Bls-MED25 were amplified based on the plasmid of GST-Bls-MED25 (L653A) mutants with corresponding primers. These proteins were expressed in wheat germ-derived cell-free protein expression system according to the previous reports (26). The obtained protein mixture was centrifuged (20,000*g* for 15 min at 4 °C), and the supernatant was used for the SDS-PAGE or AlphaScreen experiments without any purification. In the immunoblotting analyses, FLAG-tagged proteins were detected using anti-FLAG antibody (Sigma Aldrich, F1804, clone M2, 2500-fold dilution in blocking buffer) and anti-mouse IgG-HRP antibody (Southern Biotech. Inc., 1031–05, 20,000-fold dilution in blocking buffer), shown in Figures S1*A*–S3. GST-tagged proteins were detected using anti-GST-HRP conjugate (RPN1236, GE Healthcare, 5000-fold dilution in blocking buffer), shown in Figure S1*B*. Biotin-tagged proteins were detected using streptavidin-HRP conjugate (RPN1231V, GE Healthcare, 5000-fold dilution in blocking buffer), shown in Figures S4–S6.

AlphaScreen assay

AlphaScreen experiments were performed at 25 °C in the incubation buffer (50 mM Mops, pH 7.4, 50 mM NaF, 50 mM CHAPS, 0.1 mg/ml bovine serum albumin) (31). 15 μl of the reaction mixture in the incubation buffer containing 50 nM FLAG-MYC and 150 nM GST-Bls-MED25 (or GST-Bls-JAZ9) was added to a 1/2 Area AlphaPlate-96 (PerkinElmer) and incubated for 2 h at 4 °C. Subsequently, 10 μl of a detection mixture in the incubation buffer containing 0.1 μl of anti-FLAG antibody-coated AlphaScreen acceptor beads and 0.1 μl of Streptavidin-coated donor beads was added to each well. In Figure S13*B*, anti-FITC antibody-coated donor beads were used instead of Streptavidin-coated donor beads. Thereafter, the mixture was incubated for 5 h at room

temperature, and the luminescence signals were detected using the Envision 2105 Multimode Plate Reader (PerkinElmer, Inc.). The experiment was repeated three times, and the data are presented as average values with SD.

Synthesis of Biotin-MED25^{CMIDM}, Fl-MED25^{CMIDM}, Fl-JAZ10^{CMID}, Biotin-MED25$^{\alpha1\text{-}2\ loop-\alpha2}$, Biotin-MED25$^{571-612}$, and Fl-MED25$^{571-612}$

The peptides were prepared using the fully automated microwave peptide synthesizer Initiator+ Alstra (Biotage Ltd) starting from Fmoc protected amino acid-tethered Wang resin (90 μm) as previously reported, with minor modifications (32, 33). The resin was swollen in *N,N*-dimethylformamide (DMF) at 70 °C for 20 min. The Fmoc protecting group was removed by treating with 20% piperidine in DMF twice. Amino acid coupling was accomplished by mixing the resin with Fmoc protected amino acids (3 eq), 1-(7-aza-*1H*-benzotriazol-1-yl)-*N,N,N′,N′*-tetramethyluronium hexafluorophosphate (3 eq), 1-hydroxy-7-azabenzotriazole (3 eq), and DIPEA (12 eq) in DMF and subjecting it to microwave irradiation at 50 °C for either 30 min (Fmoc-Arg-OH) or 10 min (all others). After the peptide had been fully elongated, the resin was mixed with biotin or 5-carboxy-fluorescein diacetate (2 eq), 1-(7-aza-*1H*-benzotriazol-1-yl)-*N,N,N′,N′*-tetramethyluronium hexafluorophosphate (4 eq), and DIPEA (8 eq) in DMF and incubated at r.t. for 3 h. After the reaction, the peptide was deprotected by stirring in TFA solution containing thioanisole, anisole, and 1,2-ethanedithiol at r.t. for 1.5 h. The reaction mixture was purified by HPLC using a Develosil ODS-HG-5 column (Φ 4.6 × 250 mm) eluting with a linear gradient (CH_3CN (0.05% TFA):H_2O (0.05% TFA) = 20:80 (5 min) to 50:50 (35 min)) to afford biotin-conjugated or fluorescein-conjugated peptides (Biotin-MED25^{CMIDM}, Fl-MED25^{CMIDM}, and Fl-JAZ10^{CMID}). In case of Biotin-MED25$^{\alpha1\text{-}2\ loop-\alpha2}$, the reaction mixture was purified by HPLC twice using a Develosil ODS-HG-5 column (Φ 4.6 × 250 mm) eluting with a linear gradient (first round: CH_3CN (0.05% TFA):H_2O (0.05% TFA) = 40:60 (5 min) to 60:40 (35 min) and second round: CH_3CN (0.05% TFA):H_2O (0.05% TFA) = 40:60 (5 min) to 70:30 (35 min)). After lyophilization, each conjugated peptide was dissolved in sterilized water containing 1 mM tris(2-carboxyethyl)phosphine to prepare the stock solution. The concentration of the stock solution of Biotin-MED25^{CMIDM}, Biotin-MED25$^{\alpha1\text{-}2\ loop-\alpha2}$, and Biotin-MED25$^{571-612}$ were determined by the Bradford assay. The concentrations of the stock solution of Fl-MED25^{CMIDM}, Fl-JAZ10^{CMID}, and Fl-MED25$^{571-612}$ were determined by their absorbance at 494 nm in 0.1 N NaOH aqueous solution using a molar extinction coefficient of 75,000 M^{-1} cm^{-1}. The purity of each peptide was confirmed by HPLC analyses, and these were characterized by MALDI-TOF MS as follows; Biotin-MED25^{CMIDM}: m/z $[M + H]^+$ calcd for 4888.61, found 4888.60; Fl-MED25^{CMIDM}: m/z $[M + H]^+$ calcd for 5020.58, found 5020.56; Fl-JAZ10^{CMID}: m/z $[M + H]^+$ calcd for 4207.20, found 4207.20; Biotin-MED25$^{\alpha1\text{-}2\ loop-\alpha2}$: m/z $[M+Na]^+$ calcd for 1946.05, found 1946.05; Biotin-MED25$^{571-612}$: m/z $[M + H]^+$ calcd for 4934.48, found 4934.49; and Fl-MED25$^{571-612}$: m/z $[M + H]^+$ calcd for 5066.46, found 5066.46.

Synthesis of biotin-MED25$^{N\text{-}loop\text{-}\alpha1}$

Cysteine-introduced MED25$^{N\text{-}loop\text{-}\alpha1}$ peptide was prepared by the solid-phase peptide synthesis, as described above the experimental section. The crude of the deprotected peptide (1.5 μmol) was dissolved in 1 ml of 1:1 solution of 1 M Tris-HCl buffer (pH 8.0) and DMSO containing tris(2-carboxyethyl)phosphine (5 mM). The solution was mixed with biotin-maleimide (2 mg, 3.0 eq, purchased from Sigma-Aldrich, B1267) and incubated at 37 °C for 36 h. The reaction mixture was purified by HPLC using a Develosil ODS-HG-5 column (Φ 4.6 × 250 mm) eluting with a linear gradient (CH_3CN (0.05% TFA):H_2O (0.05% TFA) = 20:80 (5 min) to 50:50 (35 min)) to afford biotin-conjugated MED25$^{N\text{-}loop\text{-}\alpha1}$ peptide. After lyophilization, the peptide was dissolved in sterilized water. The concentration of the stock solution of Biotin-MED25$^{N\text{-}loop\text{-}\alpha1}$ was determined by BCA assay. The purity of the peptide was confirmed by HPLC analyses, and it was characterized by MALDI-TOF MS as follows; Biotin-MED25$^{N\text{-}loop\text{-}\alpha1}$: m/z $[M + H]^+$ calcd for 3019.47, found 3019.47.

Fluorescent anisotropy assay

Fluorescent anisotropy experiments were performed at room temperature in 20 mM Tris-HCl (pH 8.0, 200 mM NaCl, and 10% Glycerol) using a quartz cell (150 μl), as previously described. His6-SUMO-tagged MYC3 (44–238) was added dropwise to the solution containing fluorophore-conjugated peptides (Fl-MED25^{CMIDM} or Fl-JAZ10^{CMID}, 100 nM). Fluorescence anisotropy was recorded on a FP-8500 (Jasco). Excitation and emission wavelengths for fluorescein are 485 nm and 516.5 nm, respectively. Fluorescence anisotropy values (r) were calculated using the following equation: $r = (I_{VV} - G \times I_{VH})/(I_{VV} + 2G \times I_{VH})$, where I_{VV} and I_{VH} are the fluorescence intensities observed through polarizers parallel and perpendicular to the polarization of the exciting light, respectively, and G is a correction factor to account for instrumental differences in detecting emitted compounds ($G = I_{HV}/I_{HH}$). An average value of three independent measurements was calculated for each point. Anisotropy titration curves were analyzed with the nonlinear curve-fitting analysis to evaluate apparent K_a and K_d values.

Pull down assay

For the pull down assay, FLAG-MYC3 (0.5 μM) and Fl-MED25^{CMIDM} peptide (5 μM) or Fl-MED25$^{571-612}$ peptide (5 μM, as the negative control peptide that is another domain with the same length as CMIDM in MED25) in 70 μl of incubation buffer (50 mM Mops, pH 7.4, 50 mM NaF, 50 mM CHAPS, 0.1 mg/ml bovine serum albumin) was incubated at 4 °C for 2 h, and then mixed with anti-fluorescein antibody (Genetex, GTX26644, 0.5 μl). After 10 h incubation at 4 °C, the samples were mixed with Protein G magnetic beads (Bio-Rad, SureBeads Protein G Magnetic Beads, 10 μl in 50%

incubation buffer slurry). After 3 h incubation at 4 °C, the samples were washed three times with 200 μl of the incubation buffer. The washed beads were resuspended in 50 μl of SDS-PAGE loading buffer containing DTT (100 mM). After boiling for 10 min at 60 °C, the samples were subjected to SDS-PAGE and analyzed by Western blotting. The bound FLAG-MYC3 proteins were detected using anti-FLAG antibody (Sigma Aldrich, F1804, clone M2, 2500-fold dilution in blocking buffer) and anti-mouse IgG-HRP antibody (Southern Biotech. Inc., 1031–05, 20,000-fold dilution in blocking buffer), shown in Figure S10.

Data availability

All relevant data are contained in the article.

Supporting information—This article contains supporting information.

Author contributions—Y. T. and M. U. conceptualization; Y. T., A. N., H. T., and T. S. methodology; Y. T., A. N., H. T., T. S., and M. U. validation; Y. T., K. S., A. N., and H. T. formal analysis; Y. T., K. S., A. N., and H. T. investigation; Y. T., K. S., A. N., H. T., and T. S. resources; Y. T., K. S., A. N., H. T., T. S., and M. U. data curation; Y. T. and M. U. writing–original draft; Y. T. visualization; Y. T., H. T., T. S., and M. U. funding acquisition; Y. T. and M. U. project administration; Y. T., K. S., A. N., H. T., T. S., and M. U. writing–review and editing; M. U. supervision.

Funding and additional information—This work was financially supported by a Grant-in-Aid for Scientific Research from JSPS, Japan (Nos. 17H06407, 18KK0162, and 20H00402 for M.U., nos. 18H02101, 19H05283, and 21H00270 for Y. T., and 21H00287 for H. T.), JSPS A3 Foresight Program (M. U.), JSPS Core-to-Core Program Asian Chemical Biology Initiative (M. U.), and Takeda Science Foundation (Y. T.).

Conflict of interest—The authors declare that they have no conflicts of interest with the contents of this article.

Abbreviations—The abbreviations used are: Bls, biotin-ligation site; CMID, cryptic MYC-interacting domain; CMIDM, CMID-like MYC-interacting domain; COI1, CORONATINE INSENSITIVE 1; DMF, *N*,*N*-dimethylformamide; FA, fluorescence anisotropy; JA-Ile, (+)-7-iso-jasmonoyl-L-isoleucine; JAZ, jasmonate-ZIM-domain; PDA, photodiode array detector; PPI, protein–protein interaction; TFs, transcription factors.

References

1. Wasternack, C. (2007) Jasmonates: An update on biosynthesis, signal transduction and action in plant stress response, growth and development. *Ann. Bot.* **100**, 681–697
2. Wasternack, C., and Hause, B. (2013) Jasmonates: Biosynthesis, perception, signal transduction and action in plant stress response, growth and development. An update to the 2007 review in Annals of Botany. *Ann. Bot.* **111**, 1021–1058
3. Pauwels, L., Barbero, G. F., Geerinck, J., Tilleman, S., Grunewald, W., Perez, A. C., Chico, J. M., Bossche, R. V., Sewell, J., Gil, E., Garcia-Casado, G., Witters, E., Inze, D., Long, J. A., De Jaeger, G., *et al.* (2010) NINJA connects the co-repressor TOPLESS to jasmonate signalling. *Nature* **464**, 788–791
4. Pauwels, L., and Goossens, A. (2011) The JAZ proteins: A crucial interface in the jasmonate signaling cascade. *Plant Cell* **23**, 3089–3100
5. Ke, J., Ma, H., Gu, X., Thelen, A., Brunzelle, J. S., Li, J., Xu, H. E., and Melcher, K. (2015) Structural basis for recognition of diverse transcriptional repressors by the TOPLESS family of corepressors. *Sci. Adv.* **1**, e1500107
6. Chini, A., Gimenez-Ibanez, S., Goossens, A., and Solano, R. (2016) Redundancy and specificity in jasmonate signalling. *Curr. Opin. Plant Biol.* **33**, 147–156
7. Chini, A., Fonseca, S., Fernandez, G., Adie, B., Chico, J. M., Lorenzo, O., Garcia-Casado, G., Lopez-Vidriero, I., Lozano, F. M., Ponce, M. R., Micol, J. L., and Solano, R. (2007) The JAZ family of repressors is the missing link in jasmonate signalling. *Nature* **448**, 666–671
8. Thines, B., K, L., Melotto, M., Niu, Y., Ajin, M., Liu, G., Nomura, K., He, S. Y., Howe, G. A., and Browse, J. (2007) JAZ repressor proteins are targets of the SCFCOI1 complex during jasmonate signalling. *Nature* **448**, 661–665
9. Fonseca, S., Chini, A., Hamberg, M., Adie, B., Porzel, A., Kramell, R., Miersch, O., Wasternack, C., and Solano, R. (2009) (+)-7-iso-Jasmonoyl-L-isoleucine is the endogenous bioactive jasmonate. *Nat. Chem. Biol.* **5**, 344–350
10. Kastir, L., S, A. L., Staswick, P. E., He, S. Y., and Howe, G. A. (2008) COI1 is a critical component of a receptor for jasmonate and the bacterial virulence factor coronatine. *Proc. Natl. Acad. Sci. U. S. A.* **105**, 7100–7105
11. Chen, R., Jiang, H., Li, L., Zhai, Q., Qi, L., Zhou, W., Liu, X., Li, H., Zheng, W., Sun, J., and Li, C. (2012) The Arabidopsis mediator subunit MED25 differentially regulates jasmonate and abscisic acid signaling through interacting with the MYC2 and ABI5 transcription factors. *Plant Cell* **24**, 2898–2916
12. Cevik, V., Kidd, B. N., Zhang, P., Hill, C., Kiddle, S., Denby, K. J., Holub, E. B., Cahill, D. M., Manners, J. M., Schenk, P. M., Beynon, J., and Kazan, K. (2012) MEDIATOR25 acts as an integrative hub for the regulation of jasmonate-responsive gene expression in Arabidopsis. *Plant Physiol.* **160**, 541–555
13. An, C., Li, L., Zhai, Q., You, Y., Deng, L., Wu, F., Chen, R., Jiang, H., Wang, H., Chen, Q., and Li, C. (2017) Mediator subunit MED25 links the jasmonate receptor to transcriptionally active chromatin. *Proc. Natl. Acad. Sci. U. S. A.* **114**, E8930–E8939
14. Wang, H., Li, S., Li, Y., Xu, Y., Wang, Y., Zhang, R., Sun, W., Chen, Q., Wang, X. J., Li, C., and Zhao, J. (2019) MED25 connects enhancer-promoter looping and MYC2-dependent activation of jasmonate signalling. *Nat. Plants* **5**, 616–625
15. Zhai, Q., Deng, L., and Li, C. (2020) Mediator subunit MED25: At the nexus of jasmonate signaling. *Curr. Opin. Plant Biol.* **57**, 78–86
16. Liu, Y., Du, M., Deng, L., Shen, J., Fang, M., Chen, Q., Lu, Y., Wang, Q., Li, C., and Zhai, Q. (2019) MYC2 regulates the termination of jasmonate signaling via an autoregulatory negative feedback loop. *Plant Cell* **31**, 106–127
17. Koo, A. J., Cooke, T. F., and Howe, G. A. (2011) Cytochrome P450 CYP94B3 mediates catabolism and inactivation of the plant hormone jasmonoyl-L-isoleucine. *Proc. Natl. Acad. Sci. U. S. A.* **108**, 9298–9303
18. Heitz, T., Widemann, E., Lugan, R., Miesch, L., Ullmann, P., Desaubry, L., Holder, E., Grausem, B., Kandel, S., Miesch, M., Werck-Reichhart, D., and Pinot, F. (2012) Cytochromes P450 CYP94C1 and CYP94B3 catalyze two successive oxidation steps of plant hormone Jasmonoyl-isoleucine for catabolic turnover. *J. Biol. Chem.* **287**, 6296–6306
19. Koo, A. J., Thireault, C., Zemelis, S., Poudel, A. N., Zhang, T., Kitaoka, N., Brandizzi, F., Matsuura, H., and Howe, G. A. (2014) Endoplasmic reticulum-associated inactivation of the hormone jasmonoyl-L-isoleucine by multiple members of the cytochrome P450 94 family in Arabidopsis. *J. Biol. Chem.* **289**, 29728–29738
20. Moreno, J. E., Shyu, C., Campos, M. L., Patel, L. C., Chung, H. S., Yao, J., He, S. Y., and Howe, G. A. (2013) Negative feedback control of jasmonate signaling by an alternative splice variant of JAZ10. *Plant Physiol.* **162**, 1006–1017
21. Zhang, F., Ke, J., Zhang, L., Chen, R., Sugimoto, K., Howe, G. A., Xu, H. E., Zhou, M., He, S. Y., and Melcher, K. (2017) Structural insights into alternative splicing-mediated desensitization of jasmonate signaling. *Proc. Natl. Acad. Sci. U. S. A.* **114**, 1720–1725

22. Chung, H. S., Cooke, T. F., Depew, C. L., Patel, L. C., Ogawa, N., Kobayashi, Y., and Howe, G. A. (2010) Alternative splicing expands the repertoire of dominant JAZ repressors of jasmonate signaling. *Plant J.* **63**, 613–622
23. Goossens, J., Swinnen, G., Vanden Bossche, R., Pauwels, L., and Goossens, A. (2015) Change of a conserved amino acid in the MYC2 and MYC3 transcription factors leads to release of JAZ repression and increased activity. *New Phytol.* **206**, 1229–1237
24. Sheard, L. B., Tan, X., Mao, H., Withers, J., Ben-Nissan, G., Hinds, T. R., Kobayashi, Y., Hsu, F. F., Sharon, M., Browse, J., He, S. Y., Rizo, J., Howe, G. A., and Zheng, N. (2010) Jasmonate perception by inositol-phosphate-potentiated COI1-JAZ co-receptor. *Nature* **468**, 400–405
25. Zhang, F., Yao, J., Ke, J., Zhang, L., Lam, V. Q., Xin, X. F., Zhou, X. E., Chen, J., Brunzelle, J., Griffin, P. R., Zhou, M., Xu, H. E., Melcher, K., and He, S. Y. (2015) Structural basis of JAZ repression of MYC transcription factors in jasmonate signalling. *Nature* **525**, 269–273
26. Sawasaki, T., Hasegawa, Y., Tsuchimochi, M., Kamura, N., Ogasawara, T., Kuroita, T., and Endo, Y. (2002) A bilayer cell-free protein synthesis system for high-throughput screening of gene products. *FEBS Lett.* **514**, 102–105
27. Sawasaki, T., Ogasawara, T., Morishita, R., and Endo, Y. (2002) A cell-free protein synthesis system for high-throughput proteomics. *Proc. Natl. Acad. Sci. U. S. A.* **99**, 14652–14657
28. Suzuki, K., Takaoka, Y., and Ueda, M. (2021) Rational design of a stapled JAZ9 peptide inhibiting protein–protein interaction of a plant transcription factor. *RSC Chem. Biol.* **2**, 499–502
29. Li, J., Zhang, K., Meng, Y., Hu, J., Ding, M., Bian, J., Yan, M., Han, J., and Zhou, M. (2018) Jasmonic acid/ethylene signaling coordinates hydroxycinnamic acid amides biosynthesis through ORA59 transcription factor. *Plant J.* **95**, 444–457
30. Yang, Y., Ou, B., Zhang, J., Si, W., Gu, H., Qin, G., and Qu, L. J. (2014) The Arabidopsis Mediator subunit MED16 regulates iron homeostasis by associating with EIN3/EIL1 through subunit MED25. *Plant J.* **77**, 838–851
31. Melcher, K., Ng, L. M., Zhou, X. E., Soon, F. F., Xu, Y., Suino-Powell, K. M., Park, S. Y., Weiner, J. J., Fujii, H., Chinnusamy, V., Kovach, A., Li, J., Wang, Y., Li, J., Peterson, F. C., *et al.* (2009) A gate-latch-lock mechanism for hormone signalling by abscisic acid receptors. *Nature* **462**, 602–608
32. Takaoka, Y., Nagumo, K., Azizah, I. N., Oura, S., Iwahashi, M., Kato, N., and Ueda, M. (2019) A comprehensive *in vitro* fluorescence anisotropy assay system for screening ligands of the jasmonate COI1-JAZ co-receptor in plants. *J. Biol. Chem.* **294**, 5074–5081
33. Takaoka, Y., Hayashi, K., Suzuki, K., Azizah, I. N., and Ueda, M. (2020) A fluorescence anisotropy-based comprehensive method for the in vitro screening of COI1-JAZs agonists and antagonists. *Methods Mol. Biol.* **2085**, 145–160